Rapid evolution of the relativistic jet system SS 433*

V.P. Goranskij[1], E.A. Barsukova[2], A.N. Burenkov[2], A.F. Valeev[2], S.A. Trushkin[2], I.M. Volkov[1], V.F. Esipov[1], T.R. Irsmambetova[1], A.V. Zharova[1]

1- SAI, Moscow University; 2- Special Astrophysical Observatory, Russian Academy of Sciences
goray@sao.ru Vitaly Goranskij

The eclipsing system SS 433 (V1343 Aql) with moving emission lines in the spectrum consists of an A3–A7 I giant (Gies et al., 2002; Hillwig & Gies, 2004) and a neutron star (Goranskij, 2011, 2013). The moving components of Balmer and He I lines are formed by a pair of oppositely directed, highly collimated and relativistic precessing gaseous jets moving with a velocity of 0.26 c. The orbital period of 13.082 days, the jet precession period of 162 days, and the jet nodding period of 6.28 days are presented in photometric data. The star is located in the center of the W50 radio structure and interpreted as a 10000-year old supernova remnant. The distance to SS 433 is well known from radio interferometry, it is 5.12 ± 0.27 kpc.

Why the neutron star? Gies et al. (2002), Hillwig & Gies (2004) have discovered weak lines in the blue spectral region of SS 433 that belong to mass accretion donor, an A3–A7 I type star, and estimated its contribution in V band of 0.36 ± 0.07 in eclipse near T_3 precession phase. We have extracted the spectral energy distribution (SED) of A-type donor on basis of its large Balmer jump in UV, and picked out the SED of a very hot radiation source with a power spectrum by using UBVRcIc photometry in two eclipses. As a result, we estimated the absolute magnitude of A-type donor as $-5^m.9 \leq M_V \leq -5^m.0$, and reddening $E(B-V) = 2^m.65 \pm 0^m.03$. By knowing bolometric corrections, we have calculated luminosity of the donor, effective temperature, and mass based on the Mass–Luminosity dependence and evolution tracks. The donor mass is in the range between 8.3 and 11.0 $M_\odot$. Spectroscopic mass range estimate from 9.4 to 12.7 $M_\odot$ (Kubota et al., 2010) does not contradict to these values. With the value of mass ratio $q = 0.1496$ determined by Brinkman et al. (1989) with the Ginga X-ray observations of jet base eclipse (confirmed by the RXTE data), we have mass of the compact object in the range between 1.25 and 1.65 $M_\odot$. The mean value 1.45 $M_\odot$ exceeds the Chandrasekhar limit of white dwarfs and rejects the black-hole hypothesis.

What is the problem? Based on the Stephan–Boltzmann law an A5 type star with T = 8300 K and L = 10800 $L_\odot$ has R = 50 $R_\odot$ whereas the orbit radius of a binary with the mass of 1.45 + 9.7 $M_\odot$ should be of 52 $R_\odot$ according with Kepler's Third law. Even if taking into account the inaccuracy of these estimates it is clear that the system is close, contact or has a common envelope.

Observations. We have analyzed the collection of 40-year observations to find any evidences of components proximity. Unfortunately, irregular observations were not enough, so we perform synoptic monitoring of the star with the small 25-cm telescope and electronic image tube equipped with a microchannel plate. This combination gives the reaction curve close to Cousins R, and limiting magnitude of about 14.

Results. 1. Photometric 162-day periodicity caused by the precession of a circumstellar disc.
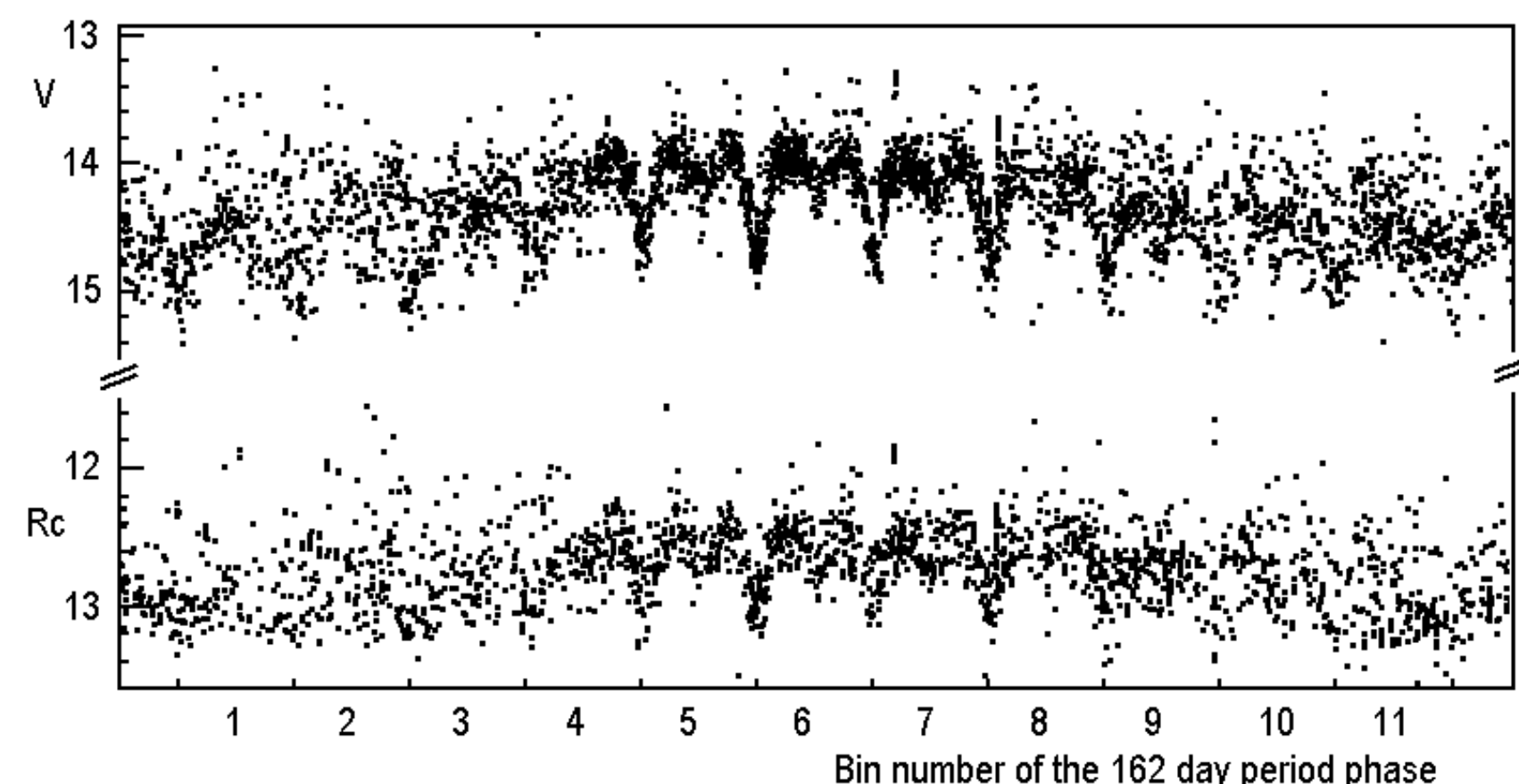

Fig. 1. Evolution of orbital light curve of SS 433 dependent on the precession phase 162-day period. In this Figure, 13-day light curves calculated in small phase bins are connected in order of increasing precession phase. The T_3 moment corresponds to the bin No.6. The binary light curve is clearly visible only near T_3. However, it is distorted or completely invisible in other precession phases. Barnes et al. (2006) explain this phenomenon with the expanding circumstellar precessing equatorial disc, which makes the donor partially visible or totally masked.

We have confirmed the presence of such a disc, and it masks the binary in the certain phases. But we think it is forming by the matter, which the system loses through the external Lagrange point L_2, and is rotating around the mass center of the system located inside the donor. Other confirmation facts of such a disk are the following: (a) the lag of photometric precession in the Rc band relative to spectroscopic T_3 phase by ~10 days (see Fig. 2); (b) the infrared excess in the R and I bands (Goranskij, 2011) which is radiated by the external parts of this disk; (c) the equatorial outflow seen at radio interferometry (Paragi et al., 1999).
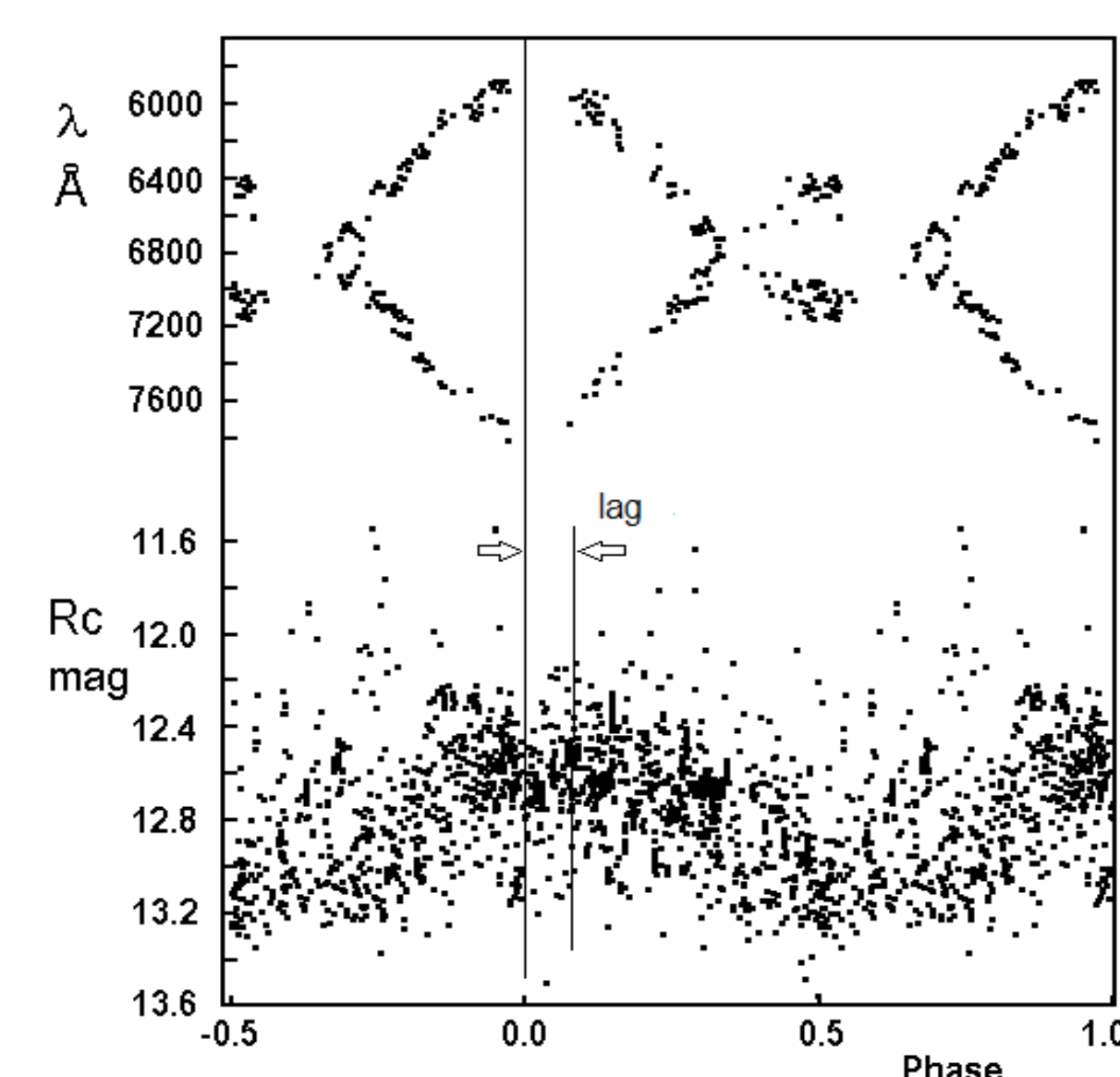

Fig. 2. Phase lag of the precession phase Rc light curve (bottom) relative to spectroscopically determined location of Hα-line relativistic components. The time range is JD 2453000 – 2458322. The linear elements of precession for this time range are $T_3 = 2454055 + 162.55$ E. The lag is due to essential contribution of external cool parts of the circumstellar disc in the R-band radiation.

2. Disappearance of the eclipses.

40 year-long observations show variability of widths and depths of eclipses (partly connected with the precession phase, with outbursts or active states), and sometimes their total lack. Our synoptic monitoring reveals some episodes (marked in Fig. 3 as Case C). One such event near the T3 precession phase in September – October 2016 began with a shallow eclipse on Sep. 6, the following two eclipses were absent. Note that such episodes happened at the increased brightness level of the system. Fig.4 shows the orbital phase light curve (the first shallow eclipse observation is marked by "1"). Here the "ellipsoidal variations" out of eclipses or any other orbital-period variations are not seen, too.

* Poster contribution to the IAU Symposium No.346 "High-mass X-ray binaries: illuminating the passage from massive binaries to merging compact objects". Vienna, August 27-31, 2018.
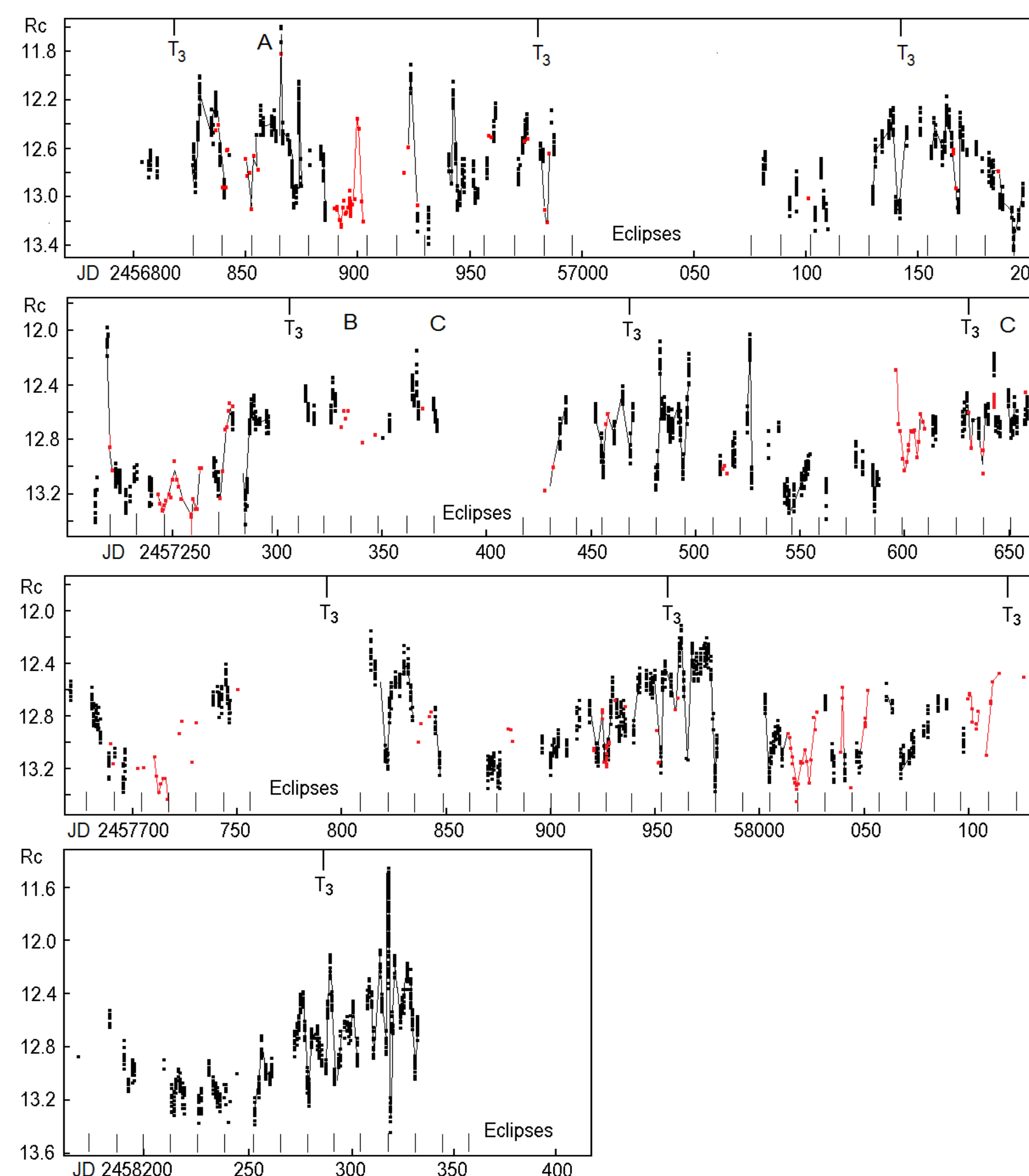

Fig. 3. The results of synoptic Rc-band monitoring of SS 433 in 2014-2018. Red points are the CCD observations. Black ones are eye estimates with the image tube. The systematic difference between these sets is $0^m.22$, and it is taken into account. T_3 moments are calculated with the following formula: $T_3 = 2454055 + 162.55$ E.
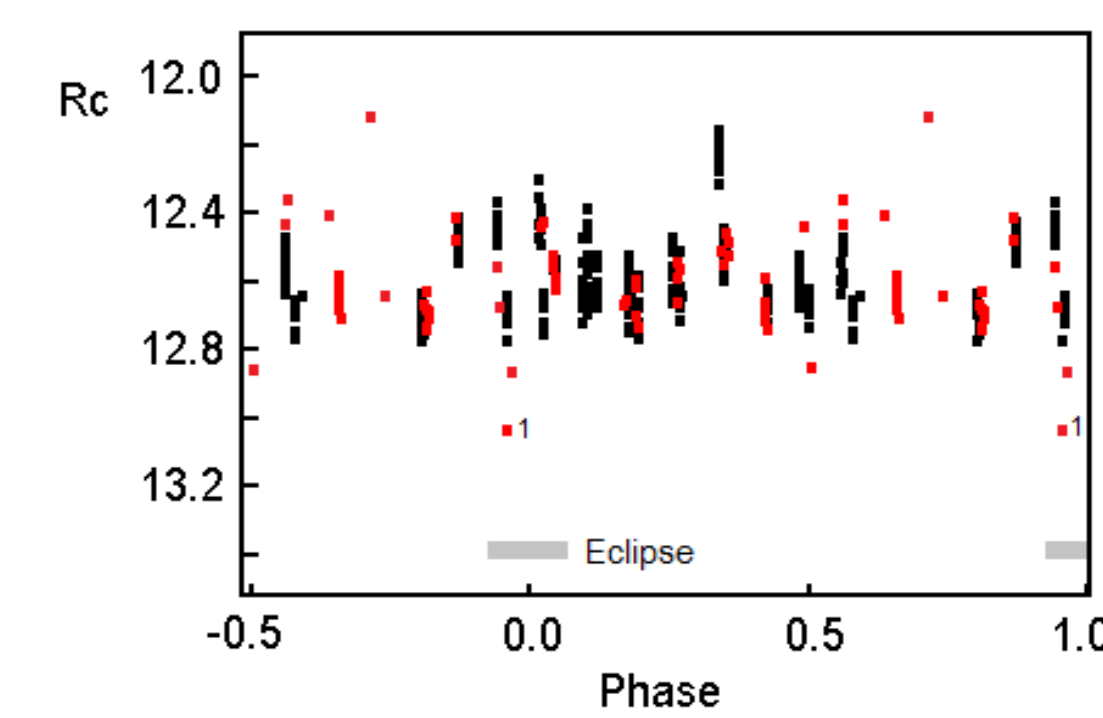

Fig. 4. The light curve of SS 433 plotted versus phase of the orbital elements Min I = 2450023.83 + 13.082454 · E. Observations relate to the time range between Aug 26 and Oct 8, 2016. "1" – the first shallow eclipse in the episode.

We explain this episode as the formation of the common envelope of the A type star with the neutron star inside. The envelope radius was larger than the radius of the A-star's Roche lobe, and therefore the envelope could not be masked by the external circumstellar disk at the wide range of precessing phases around T_3 (Case B in Fig. 3). When the neutron star is inside of the common envelope with the A-star, it has nothing to eclipse. On 2016 October 8.76 UT we have taken a spectrum of SS433 with the SAO 1-m Zeiss telescope and UAGS spectrograph. The relativistic components of Hα were visible in the spectrum, so the jets were not blocked in this episode.

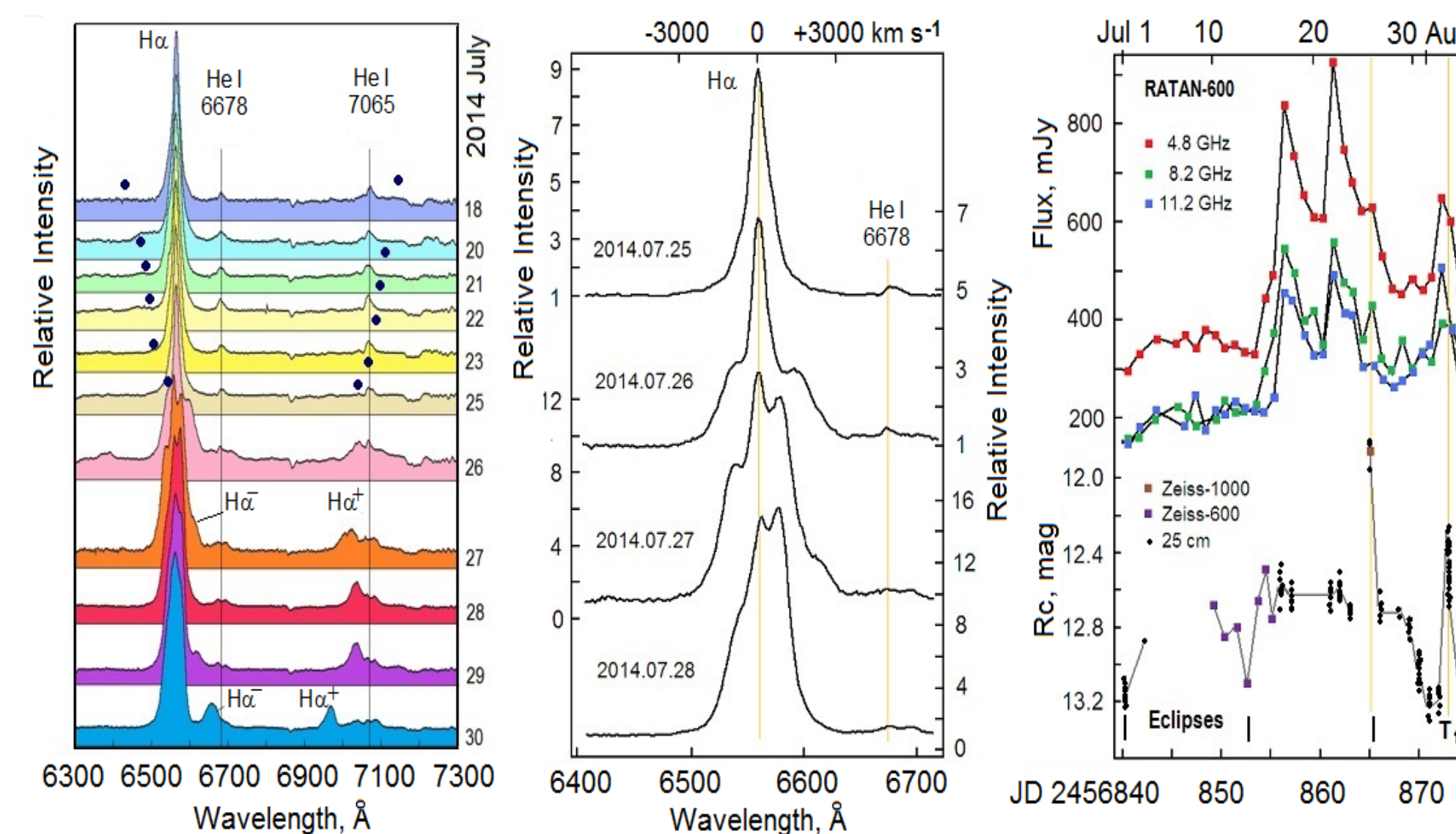### 3. Event of the common envelope ejection and the recovery of jets.

Fig. 5. In July 26, 2014, we observed a powerful outburst of SS 433 with an unusually strong infrared excess in eclipse (Goranskij & Spiridonova, 2014; Charbonell et al., 2014). Fortunately, the observations were accompanied by daily multi-frequency monitoring with the RATAN-600 radio telescope, and spectroscopy by V.F. Esipov with 125-cm telescope at the SAI Crimean Station. Additional spectra in the outburst and after it were described by Charbonnel et al. In Esipov's spectra obtained during 6 days before the outburst, the relativistic lines are invisible, it means that jets were blocked. Their forthcoming locations of lines are marked by black circles. In outburst, Hα profile showed a narrow central component and wide pedestal with FWZI ~ 7000 km s^{-1}. Charbonell et al. describe this profile as three-component one, and note its rapid variability. At the outburst, the relativistic lines reappeared at the forthcoming places. Fig 5 (left) shows that the Hα$^-$ component superimposed on the Hα line profile, and its motion can explain the variability of the pedestal. In a few days, the intensity of the pedestal increased gradually with decreasing its width, the central component weakened, and then brightness of the star went down to the normal level for the T_1 precession phase (Fig. 5, right).

Taking into account the strong IR excess in the outburst it becomes clear that this event was the ejection of the large mass envelope accompanied by the jets' recovery (Case A, Fig. 3). The expanding envelope interacted with the stellar wind.

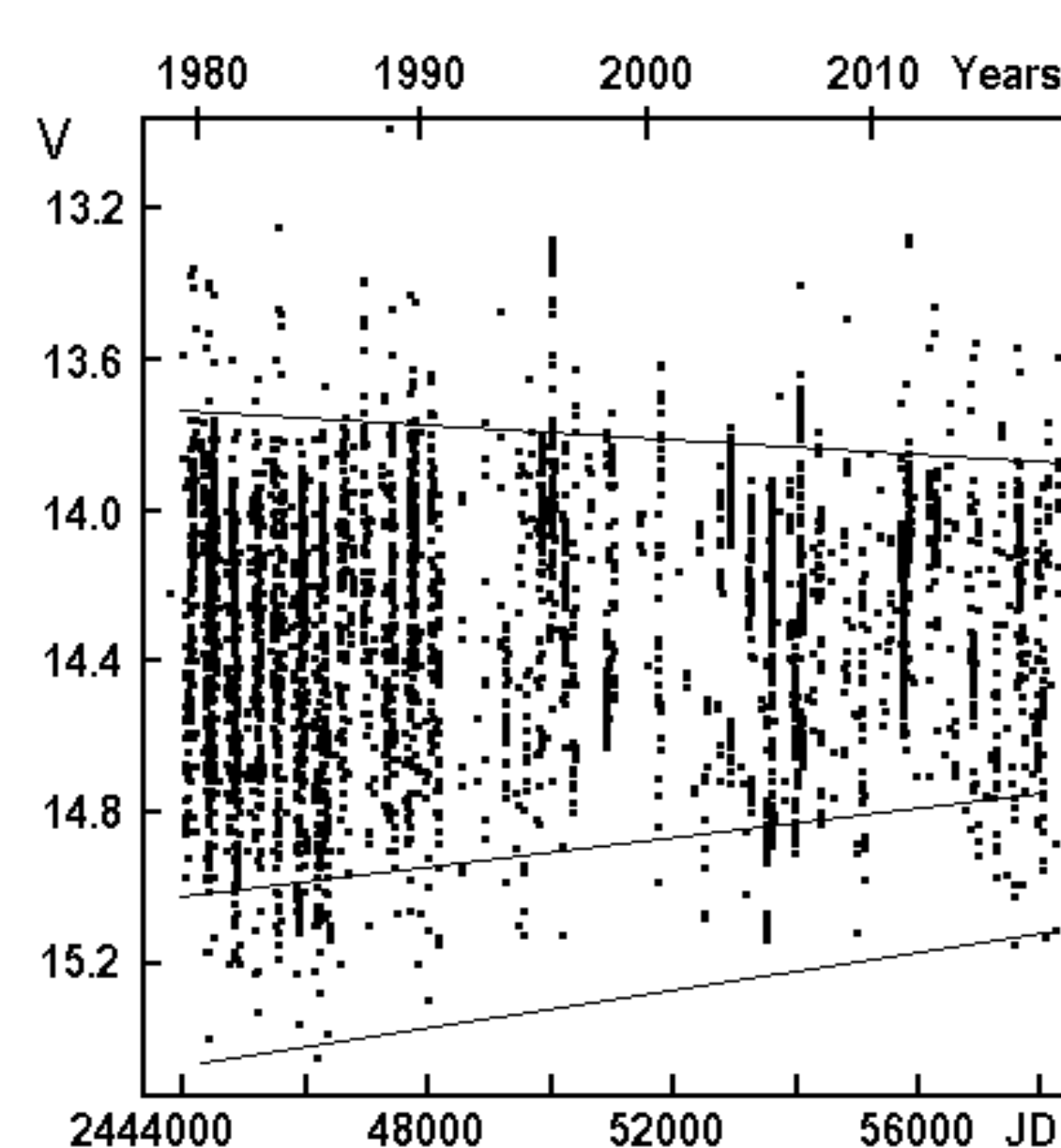### 4. Secular changes of the light curve for 40 years.

Fig. 6. This Figure shows that the amplitudes of all three periodic variations are decreasing gradually during 40 years of observations. The amplitudes decrease due to increasing donor's radius and brightness. Probably, this process is irregular and spasmodic.
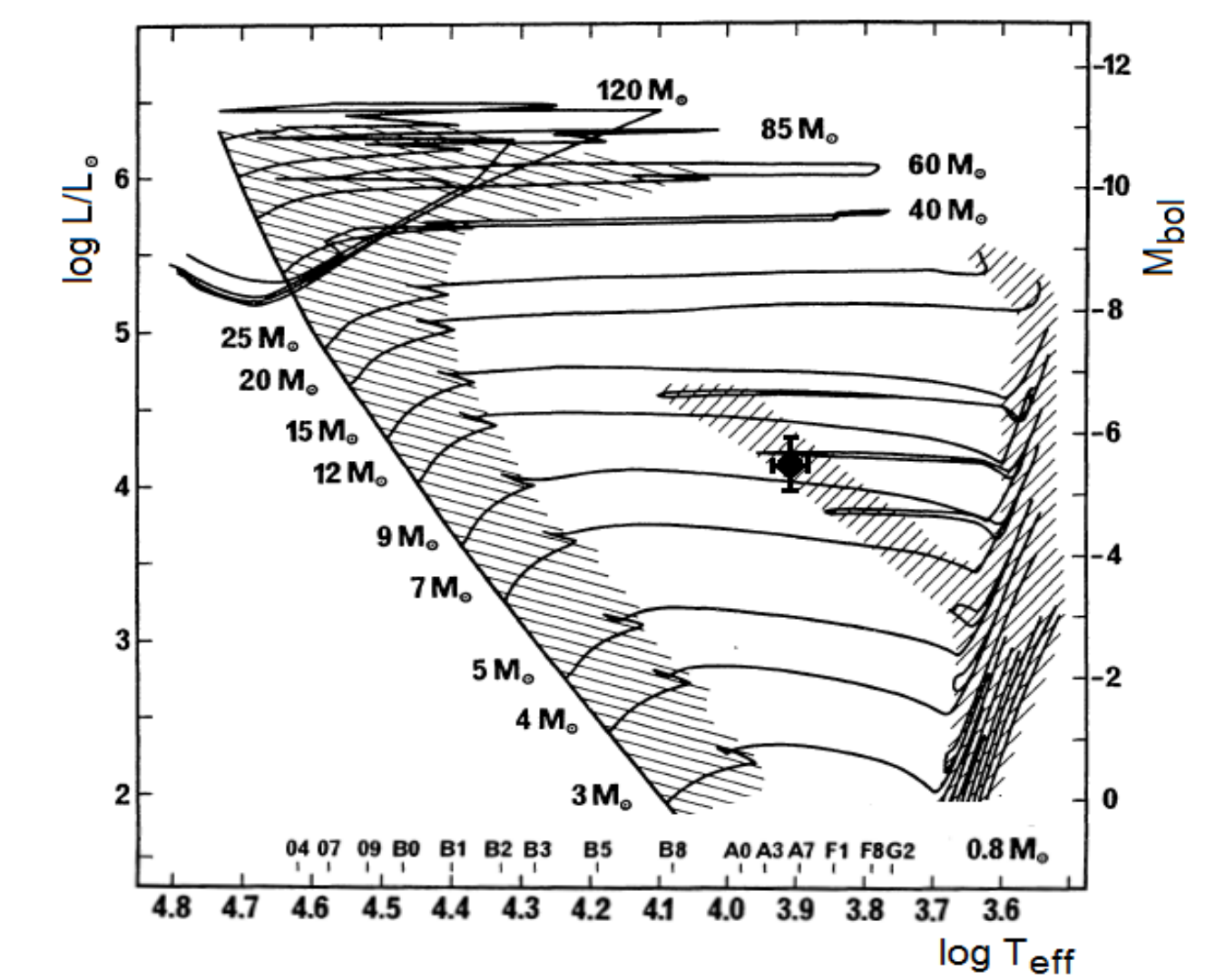

Fig. 7. Location of the SS 433 donor in the Temperature-Luminosity diagram. Tracks are from Schaller et al. (1992). The star is on the way to red giants, and its shell expands being truncated by the Roche lobe. Mass transfer from the A-type donor passes into a dynamical timescale. Overfilling of the neutron star's Roche lobe and sporadic events of common envelope formation interrupted by ejections of a large mass volume become more frequent.

Podsiadlowski (2014) about dynamical mass transfer:

"Mass transfer is unstable when the accreting star cannot accrete all the material transferred from the donor star. The transferred material than piles up on the accretor and starts to expand, ultimately filling and overfilling the accretor's Roche lobe. This leads to the formation of a common-envelope (CE) system, where the core of the donor and the companion form a binary immersed in the envelope of the donor star. This typically happens when the donor star is a giant or supergiant with a convective envelope, since a star with a convective envelope tends to expand rather than shrink when it loses mass very rapidly (adiabatically), while the Roche-lobe radius shrinks when mass is transferred from a more massive to a less massive star; this makes the donor overfill its Roche lobe by an ever larger amount and causes runaway mass transfer on a dynamical timescale (so-called dynamical mass transfer)".

When the Roche lobe of the neutron star is filled or overfilled, the accretion gainer represents a rotating star with the neutron star in the center, i.e. a Thorne-Zytkow (1977) object.

5. SS 433 in the past, in the present and in the future.

The past. The most massive primary star of the primordial binary with the main-sequence components has passed its way to giants with the helium core. It fills and overfills its Roche lobe, transfer the most part of its mass to the less massive secondary companion, and exploded as a SN Ia (the radio structure W50 is probably a remnant of this SN). There was a Be/X-ray binary as a result. The evolution of the massive secondary star accelerates to fill its Roche lobe, and to become the accretion donor backwards to the neutron star.
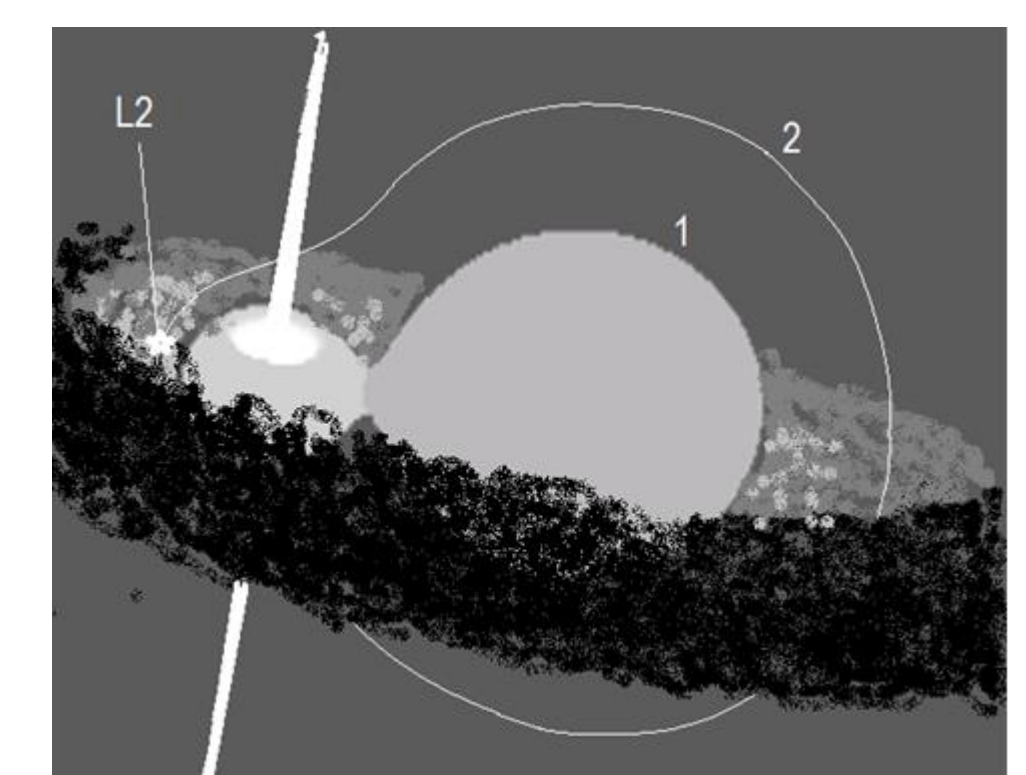

Fig. 8. Schematic view of SS 433 system at present time with different degree of overfilling Roche lobe and different modes of common envelope formation.

The present. The transfer of mass from the donor turns to dynamic mode filling and overfilling the Roche lobe of the neutron star from time to time. Jets are forming inside the neutron star's envelope created from the accreted matter, and burst through channels and nozzles, which are seen as bright spots on the surface of the photosphere. The visibility conditions of nozzles take essential contribution in the light curve with the periodic nutation wave with the amplitude of $0^m.22$ and with the period P = 6.28884 days. The system loses its mass through external Lagrangian points L_2 and stellar wind. This is a short-time stage connected with the approach of the neutron star with the expanding photosphere of the donor.

The future. The neutron star will be engulfed inside a common envelope with the expanding A-type donor. Jets will be blocked and finally disappear. Then the neutron star will spiral to the center of this star and form a single star, a massive Thorne-Zytkow object. Cherepashchuk (2014) has predicted two scenarios of this development depending on the mode of accretion of matter on the central neutron star. (1) Lower-temperature mode when neutrinos do not carry the accretion energy out. This will be a luminous star at the Eddington limit with the lifetime of about $10^6 - 10^8$ years. (2) High-temperature accretion mode when neutrinos take all the accretion energy away. The lifetime of such envelope is very short, about dynamical time. Then, if it is massive enough, a single black hole will arise. The one more scenario is (3) the explosion of donor as a supernova before the merger of its nucleus with a neutron star. The remnant may be a binary of neutron stars or a binary of neutron star with a black hole.

References.
Barnes, A.D., Casares, J., Charles, P.A., et al., MNRAS **365**, 296, 2006.
Gies, D.R., Huang, W., McSwain, M.V., ApJ **578**, L67, 2002.
Charbonnel, S., Garde, O., Edlin, J., ATel #6355, 2014.
Cherepashchuk, A.M., in *Close Binary Stars*, Part II, FizMatLit, p.264, 2013 (Rus).
Goranskij V.P., Variable Stars **31**, No.5, 2011.
Goranskij, V.P., Central European Astrophys. Bull. **37**, No.1, 251.
Goranskij, V.P. & Spiridonova, O.I., ATel #6347, 2014.
Hillwig, T.C., Gies, D.R., Huang, W., et al. ApJ **615**, 422, 2004.
Kubota, K., Ueda, Y., Fabrika, S., et al., ApJ **709**, 1374, 2010.
Paragi, Z., Vermeulen, R.C., Fejes, I. et al., AsAp **348**, 910, 2010.
Podsiadlowski, P., in *Accretion Processes in Astrophysics*, Cambridge Univ. Press, p.45, 2014.
Schaller, G., Schaerer, D., Meynet, G, Maeder, A., AsAp Suppl. Ser. **96**, 269, 1992.
Thorne, K.S. & Zytkow, A.N., ApJ **212**, 832, 1977.